

Anticancer Activities of Cdc25 Phosphatase Inhibitors in the Proliferation of Human Lung Cancer Cells

Ji Yea Kim, Eun Joo Lee,[†] Chun Jaih Ryu,^{*} and Hwangseo Park^{*}

Department of Bioscience and Biotechnology, Sejong University, Seoul 143-747, Korea

^{*}E-mail: cjryu@sejong.ac.kr (C.J. Ryu); hspark@sejong.ac.kr (H. Park)

[†]College of Pharmacy and Wonkwang Oriental Medicines Research Institute, Wonkwang University, Iksan, Jeonbuk 570-749, Korea

Received November 21, 2013, Accepted November 23, 2013

Key Words : Anticancer agent, Cdc25 phosphatase, Cell permeability, Inhibitor, Lung cancer

Cell division cycle 25 (Cdc25) dual-specificity phosphatases catalyze the hydrolysis of phosphorylated threonine and tyrosine residues in proteins, and serve as key regulators of the cell division and the cell response to DNA damage.^{1,2} Of the three isoforms of Cdc25 phosphatases (Cdc25A, Cdc25B, and Cdc25C) encoded in human genome, Cdc25A acts on the control of G₁-to-S and G₂-to-M transitions in cell cycle whereas Cdc25B is mainly responsible for regulating the progression at the G₂-to-M transition.³ Related with the oncogenic properties of Cdc25A and B, several lines of experimental evidence have been provided for the involvement of Cdc25A and B in various human cancers.^{4,5} The impairment of their catalytic ability by small-molecule inhibitors can therefore be an effective strategy for the development of anticancer therapeutics.

As reviewed comprehensively in the literature,^{6,7} a great deal of efforts have been devoted to the discovery of structurally diverse Cdc25 phosphatase inhibitors through the high throughput screening,⁸ the generation of the improved derivatives of pre-existing inhibitor scaffolds,⁹⁻¹¹ and the structure-based virtual screening approaches.^{12,13} Binding modes of the novel Cdc25 inhibitors have also been addressed to gain structural insight into their inhibitory mechanisms.¹⁴ In the previous studies, we attempted to identify

novel classes of Cdc25 phosphatase inhibitors based on the virtual screening with docking simulations¹⁵ and *de novo* design methods.¹⁶ These computer-aided drug-design approaches resulted in the discovery of **1-8** shown in Figure 1, which exhibited micromolar inhibitory activities against both Cdc25A and B.

In the present study, we investigate the presence of anticancer activities of **1-8** by cell proliferation assays, and address the possibility that they can serve as a new lead compound for the development of anticancer medicine. Among the various cancers caused by Cdc25A and B, we focus our interest on the lung cancer because a common inhibitor of Cdc25A and B was shown to cause the cell cycle arrest in the G₁ phase in human lung cancer cells.¹⁷

1-8 were tested for having antitumor activity against the two non-small cell lung carcinoma (NSCLC) cell lines including NCI-H23 (H23) and A549. Both cancer cell lines were cultured in RPMI-1640 medium containing 10% fetal bovine serum (FBS) and antibiotic-antimycotic solution. To estimate the selectivity for the inhibition of cancer cell proliferation, cytotoxicities of **1-8** were also measured using normal lung fibroblast (MRC5) cells cultured in DMEM medium supplemented with 10% heat-inactivated FBS and antibiotic-antimycotic solution.

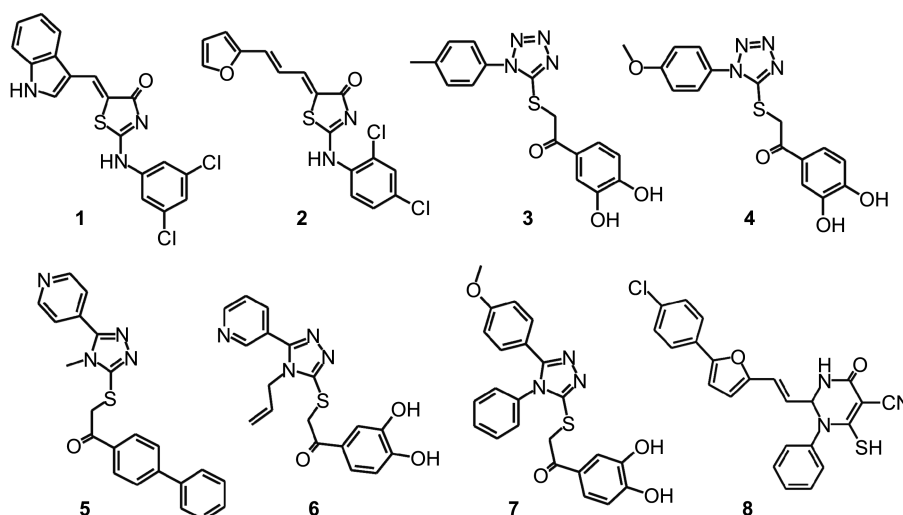


Figure 1. Chemical structures of Cdc25 phosphatase inhibitors under investigation.

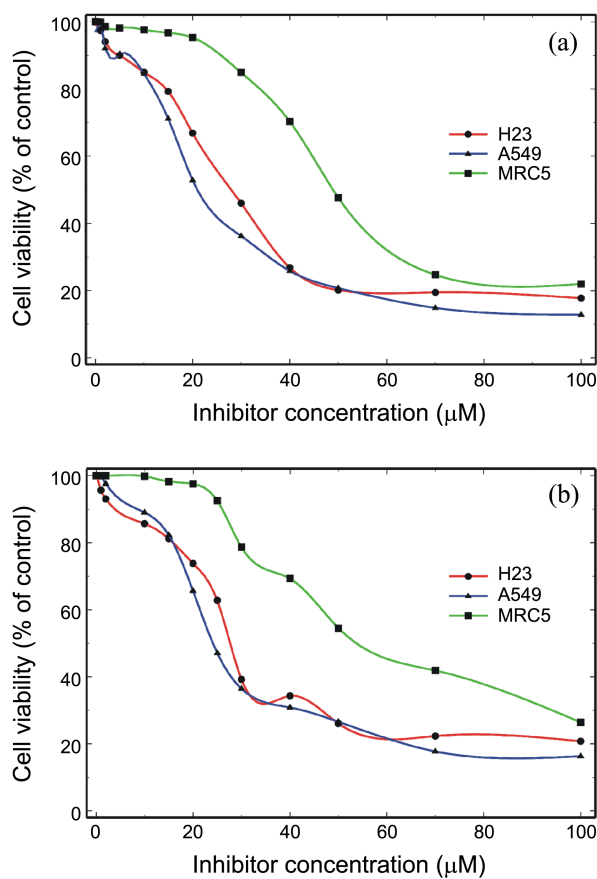
Table 1. IC₅₀ (in μM) values of **1** and **2** associated with the anticellular activities for the lung cancer (H23 and A549) and normal lung fibroblast cell lines (MRC5)

	H23	A549	MRC5
1	20.1	20.1	40.2
2	20.2	15.1	40.0

To prepare each cell line required in the cell-based assays, cells were seeded in 96-well plates at the densities of 4×10^3 , 3×10^3 , and 5×10^3 cells/well for H23, A549, and MRC5 cell lines, respectively. After the culture for 24 h, compounds **1-8** were added at various concentrations and cultured further for 72 h. Cell counting kit-8 (CCK-8) was then added to each well to estimate the number of viable cells in the cell lines. The number of viable cells was determined by measuring the absorbance at the wavelength of 450 nm with a microplate reader. The anticellular activities of the Cdc25 phosphatase inhibitors for the three cell lines were measured in triplicate at the concentrations of 1, 2, 5, 10, 15, 20, 30, 40, 50, 70, and 100 μM to obtain the dose-response curve fits. The IC₅₀ values for the three cell lines were then determined from direct regression analysis using the four-parameter sigmoidal curve.

At first, compounds **1** and **2** were found to inhibit the proliferation of H23 and A549 cell lines by more than 50% at the concentration of 20 μM whereas no significant inhibitory activity was observed for **3-8** at the same concentration. Therefore, **1** and **2** were selected for further analysis in cell proliferation assays. Table 1 lists the IC₅₀ values of **1** and **2** with respect to H23, A549, and MRC5 cell lines. Also, the dose-response behaviors of **1** and **2** measured for the three cell lines are shown in Figure 2. **1** appears to inhibit the growth of H23 and A549 cell lines with the same IC₅₀ value of 20.1 μM. On the other hand, **2** reveals a little higher inhibitory activity for A549 with the IC₅₀ value of 15.1 μM than for H23 cell line with IC₅₀ value of 20.2 μM. Interestingly, the anticellular activities of **1** and **2** with respect to the normal MRC5 cell line are found to be lower than those for the lung cancer cell lines by a factor of two. Judging from the moderate anticancer activity and selectivity, **1** and **2** deserve consideration for further development to optimize the anticancer activities.

Because the inhibitor potencies of **1-8** against Cdc25 phosphatases are similar,^{15,16} the difference in their inhibitory activities for the proliferation of various cell lines may be attributed to the difference in the permeability for cell membrane. In this regard, ClogP value has been considered as a good physicochemical property to estimate the membrane permeability of organic molecules. ClogP values of **1**, **2**, **3**, **4**, **5**, **6**, **7**, and **8** are found to be 5.56, 5.35, 2.70, 2.46, 3.30, 1.62, 4.38, and 5.70, respectively, which indicates that **1** and **2** are more hydrophobic than **3-7**. This is consistent with the higher cellular activities of **1** and **2** than **3-7** because the former is expected to transmit the cell membrane more easily than the latter. However, the difference in ClogP values may be insufficient by itself to explain the lack of cytotoxic activity

**Figure 2.** Dose-response curves of (a) **1** and (b) **2** for the inhibition of H23, A549, and MRC5 cell lines.

for **3-7** because the ClogP values were estimated with simple theoretical model instead of the experimental measurements. It should also be noted that **8** has no anticellular activity despite having the higher ClogP value than **1** and **2**, which necessitates further investigation for the membrane permeabilities of **1-8**.

Recently it was shown that the intentional introduction of hydrogen bond donor-acceptor pairs in molecules could improve the membrane permeability while retaining other favorable drug-like properties.¹⁸ Therefore we examined the presence of the intramolecular hydrogen bond in the molecular structures of **1-8** based on the quantum chemical calculations. To obtain the energy-minimized structures, we carried out the geometry optimizations through the density functional calculations. Figure 3 shows the structures of **1**, **2**, **6**, and **8** optimized at B3LYP/6-31G* level of theory. We note that the -NH- group of **1** and **2** bridging the terminal phenyl and the central thiazol-4-one ring establishes a weak hydrogen bond with the neighboring carbonyl group on the thiazol-4-one ring with the associated N-H...N hydrogen bond distances of 2.36 and 2.37 Å, respectively. These intramolecular hydrogen bonds seem to have an effect of increasing the hydrophobicity of **1** and **2** in the hydrophobic environment of cell membrane by shielding the two polar groups.

On the other hand, no intramolecular hydrogen bond is

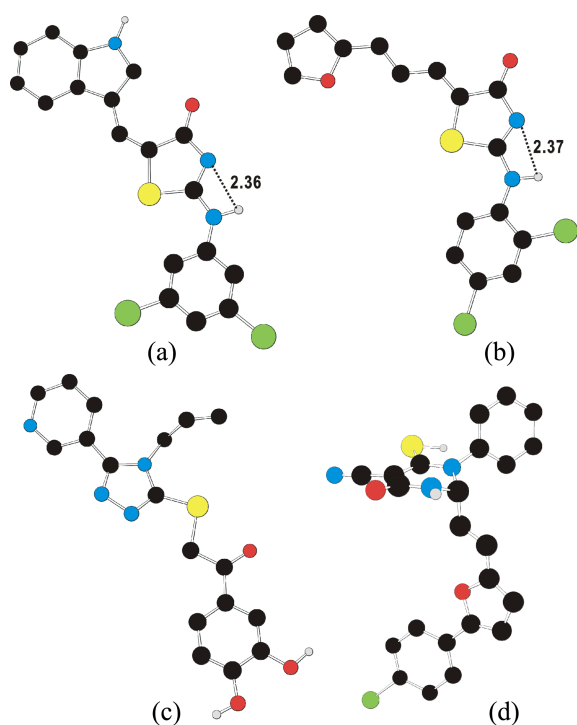


Figure 3. The energy-minimized structures of (a) **1**, (b) **2**, (c) **6**, and (d) **8** obtained with quantum chemical calculations at B3LYP/6-31G* level of theory.

established in the optimized structure of **6** (Figure 3(c)) because both terminal phenolic groups point outward with respect to the rest of the whole molecular structure and stay distant from the hydrogen bond accepting groups. This structural feature is also observed in the optimized structures of **3**, **4**, and **7** (structures are not shown), which is not surprising for their structural similarities. No hydrogen bond is found as well in the optimized structure of **8** (Figure 3(d)) in which both hydrogen bond donor groups (thiol and amidic moieties) are directed to the external bulk instead of the hydrogen bond accepting groups. Thus, the differences in conformational preferences between the molecules indicate the higher membrane permeability of **1** and **2** than **3-8**, which may culminate in the loss of anticellular activity in going from the former to the latter. The experimental and computational results found in this study confirm that a proper shielding of hydrophilic moieties by introducing the intramolecular hydrogen bonds

can be a viable means to improve the poor membrane permeability of molecules.

Acknowledgments. This work was supported by Basic Science Research Program through the National Research Foundation of Korea funded by the Ministry of Education, Science and Technology (2011-0022858 to HP), and by the Converging Research Center Program funded by the Ministry of Education, Science and Technology (Project No. 2012K001480 to CJR).

References

1. Nilsson, I.; Hoffmann, I. *Prog. Cell Cycle Res.* **2000**, *4*, 107.
2. Boutros, R.; Dozier, C.; Ducommun, B. *Curr. Opin. Cell Biol.* **2006**, *18*, 185.
3. Rudolph, J. *Biochemistry* **2007**, *46*, 3595.
4. Boutros, R.; Lobjois, V.; Ducommun, B. *Nat. Rev. Cancer* **2007**, *7*, 495.
5. Kristjansdottir, K.; Rudolph, J. *Chem. Biol.* **2004**, *11*, 1043.
6. Lavecchia, A.; Di Giovanni, C.; Novellino, E. *Mini. Rev. Med. Chem.* **2012**, *12*, 62.
7. Contour-Galcera, M. O.; Sidhu, A.; Prevost, G.; Bigg, D.; Ducommun, B. *Pharmacol. Ther.* **2007**, *115*, 1.
8. Lazo, J. S.; Aslan, D. C.; Southwick, E. C.; Cooley, K. A.; Ducruet, A. P.; Joo, B.; Vogt, A.; Wipf, P. *J. Med. Chem.* **2001**, *44*, 4042.
9. Sarkis, M.; Tran, D. N.; Kolb, S.; Miteva, M. A.; Villoutreix, B. O.; Garbay, C.; Braud, E. *Bioorg. Med. Chem. Lett.* **2012**, *22*, 7345.
10. Brault, L.; Denancé, M.; Banaszak, E.; Maadidi, S. E.; Battaglia, E.; Bagrel, D.; Samadi, M. *Eur. J. Med. Chem.* **2007**, *42*, 243.
11. Huang, W.; Li, J.; Zhang, W.; Zhou, Y.; Xie, C.; Luo, Y.; Li, Y.; Wang, J.; Li, J.; Lu, W. *Bioorg. Med. Chem. Lett.* **2006**, *16*, 1905.
12. Montes, M.; Braud, E.; Miteva, M. A.; Goddard, M. L.; Mondesert, O.; Kolb, S.; Brun, M. P.; Ducommun, B.; Garbay, C.; Villoutreix, B. O. *J. Chem. Inf. Model.* **2008**, *48*, 157.
13. Kolb, S.; Mondesert, O.; Goddard, M. L.; Jullien, D.; Villoutreix, B. O.; Garbay, C.; Braud, E. *ChemMedChem* **2009**, *4*, 633.
14. Lavecchia, A.; Cosconati, S.; Limongelli, V.; Novellino, E. *ChemMedChem* **2006**, *1*, 540.
15. Park, H.; Bahn, Y. J.; Jung, S.-K.; Jeong, D. G.; Lee, S.-H.; Seo, I.; Yoon, T.-S.; Kim, S. J.; Ryu, S. E. *J. Med. Chem.* **2008**, *51*, 5533-5541.
16. Park, H.; Bahn, Y. J.; Ryu, S. E. *Bioorg. Med. Chem. Lett.* **2009**, *19*, 4330.
17. Aoyagi, Y.; Masuko, N.; Ohkubo, S.; Kitade, M.; Nagai, K.; Okazaki, S.; Wierzba, K.; Terada, T.; Sugimoto, Y.; Yamada, Y. *Cancer Sci.* **2005**, *96*, 614.
18. Rafi, S. B.; Hearn, B. R.; Vedantham, P.; Jacobson, M. P.; Renslo, A. R. *J. Med. Chem.* **2012**, *55*, 3163.